Archivum Immunologiae et Therapiae Experimentalis
74, 14 (2026), DOI: 10.2478/aite-2026-0014

ORIGINAL

Saccharomyces cerevisiae β-Glucan Training Induces a Nonclassical PGE_2–^{High}/NO–^{Low} Macrophage Phenotype in Response to *Pseudomonas aeruginosa* Exopolysaccharide

Marta Ciszek-Lenda[1,a] · Grzegorz Majka[1]✉ · Maciej Suski[2,3] · Sabina Górska[4] · Edyta Golińska[5] · Izabela Siemińska[6] · Rafał Olszanecki[2] · Magdalena Strus[5] · Janusz Marcinkiewicz[6,a]

Abstract

Exopolysaccharide (EPS), a major constituent of *Pseudomonas aeruginosa* biofilms, protects bacteria from M1-macrophage-mediated clearance while promoting chronic inflammation. This study investigated how *Saccharomyces cerevisiae* β-glucan (BG)-induced macrophage training reshapes subsequent inflammatory and antimicrobial responses to EPS. Peritoneal macrophages from C57BL/6 mice were trained *in vitro* with BG and subsequently stimulated with EPS purified from a clinical *P. aeruginosa* isolate obtained from a patient with severe cystic fibrosis. Cytokines, prostaglandin E_2 (PGE_2), and nitric oxide (NO) were quantified, and global proteomic profiling was performed. BG training amplified EPS-induced secretion of TNF-α, IL-6, and additional pro-inflammatory mediators. Trained macrophages also showed markedly increased PGE_2 production, minimal NO release, and reduced phagocytic activity. Proteomic analyzes confirmed upregulation of PGE_2-biosynthetic enzymes and suppression of inducible NO synthase, along with enhanced expression of antimicrobial and immunoregulatory factors, including platelet factor 4, antileucoproteinase, C1q components, and selected chemokines. These data reveal a previously uncharacterized macrophage state—neither M1 nor M2—emerging specifically from BG training and defined by high PGE_2 and low NO production in response to EPS. *S. cerevisiae* BG training reprograms EPS-stimulated macrophages toward a distinct, non-classical trained-immunity phenotype characterized by elevated PGE_2 and suppressed NO production. This newly defined phenotype represents a novel form of trained immunity and highlights the dual proinflammatory and immunoregulatory roles of macrophage-derived PGE_2. These findings suggest that targeted macrophage reprogramming may offer a promising therapeutic strategy for mitigating *P. aeruginosa* biofilm-driven chronic inflammation, including in cystic fibrosis.

Keywords
Trained macrophages • Inflammation • *P. aeruginosa* EPS • *Saccharomyces cerevisiae* β-glucan • PGE_2 • NO

Received: 16 December 2025 / Accepted: 25 February 2026 /

1. Introduction

Exopolysaccharides (EPS) are high-molecular-weight polysaccharides secreted by a wide range of microorganisms, including bacteria, fungi, and algae (Ciszek-Lenda 2011; El-Mahdy et al. 2023; Carey et al. 2024; Li et al. 2024). These complex carbohydrate molecules play diverse biological roles, such as promoting biofilm formation, protecting microbes from environmental stresses, and facilitating immune evasion. In bacterial infections, EPS are particularly important due to their dual role in enhancing pathogenicity and modulating host immune responses (Pompilio et al. 2015; Vestby et al. 2020). In the context of bacterial surface structures, it is important to distinguish EPS from lipopolysaccharides (LPS), as both contribute to microbial pathogenicity yet differ substantially in composition, localization, and biological impact. EPS are secreted into the surrounding environment or associated with the outer cell surface, where they promote adhesion, protect bacteria from environmental stressors, and shape the biofilm matrix, thus supporting persistence and immune modulation. In contrast, LPS are structurally distinct glycolipids embedded in the outer membrane of Gram-negative bacteria; they consist of lipid A, an oligosaccharide core, and an O-antigen chain, and are essential for membrane stability, resistance to antimicrobial agents, and potent activation of innate immune receptors, such as TLR4. While both EPS and LPS influence immune interactions, their immunological signatures diverge greatly: EPS often contribute to chronic, biofilm-associated immune evasion, whereas LPS act as strong endotoxins capable of inducing robust cytokine release and, in severe circumstances, septic shock. Thus, EPS and LPS, despite sharing polysaccharide components, fulfill highly distinct and non-redundant roles in microbial ecology and host-pathogen interactions (Wang et al. 2023).

[a]*Co-first authors*

[1]*Department of Immunology, Faculty of Medicine, Jagiellonian University Medical College, Krakow, Poland*
[2]*Department of Pharmacology, Faculty of Medicine, Jagiellonian University Medical College, Krakow, Poland*
[3]*Proteomics Laboratory, Center for the Development of Therapies for Civilization and Age-Related Diseases, Jagiellonian University Medical College, Krakow, Poland*
[4]*Department of Microbiology, Laboratory of Microbiome Immunobiology, Hirszfeld Institute of Immunology and Experimental Therapy, Polish Academy of Sciences, Wroclaw, Poland*
[5]*Department of Infectious Diseases and Public Health, Faculty of Veterinary Medicine, University of Agriculture in Cracow, Krakow, Poland*
[6]*Faculty of Veterinary Medicine, University of Agriculture, Krakow, Poland*

✉ *grzegorz.majka@uj.edu.pl*

P. aeruginosa, an opportunistic pathogen, produces EPS, which are critical for its ability to establish chronic infections. These molecules contribute to biofilm formation, antibiotic resistance, and evasion of host defenses, rendering infections particularly challenging to treat. Furthermore, the hyperinflammatory properties of certain EPS exacerbate tissue damage by inducing excessive immune responses, often resulting in severe clinical outcomes in infections such as cystic fibrosis and chronic wound infections (Ciszek-Lenda et al. 2019; Chung et al. 2023). In our previous work, we showed that biofilm matrix components, like EPS, stimulate phagocytes to display strong proinflammatory secretory properties. These results may suggest that *in vivo,* high concentrations of biofilm components convert infiltrating phagocytes into cells responsible for tissue injury without direct contact with bacteria and phagocytosis. Hence, the interaction between biofilm and immune cells might favor chronic inflammation rather than effective killing of pathogens and resolution of inflammation (Ciszek-Lenda et al. 2023). On the contrary, emerging research highlights the potential to leverage immune training as a therapeutic strategy to combat infections. Macrophage training, a phenomenon where innate immune cells are "trained" to respond more effectively to subsequent infections, represents a promising avenue. It has been postulated that trained immunity involves epigenetic and metabolic reprograming of macrophages, leading to enhanced cytokine production, phagocytosis, and pathogen clearance (Dagenais et al. 2023; Ochando et al. 2023). One of the promising agents in macrophage training is *S. cerevisiae* β-glucan (BG), which shows immunomodulatory potential (Murphy et al. 2020; Zhong et al. 2023). In our previous work, we have demonstrated that BG enhanced the ability of macrophages to mount robust responses against pathogen *P. aeruginosa.* (named PA57) For example, in the *in vitro* tests, trained macrophages increased their production of tumor necrosis factor (TNF)-α, interleukin (IL)-6, and prostaglandin E_2 (PGE_2), but reduced secretion of IL-10 after restimulation with whole PA57 cells. Thus, it is possible that training murine macrophages with *S. cerevisiae* BG before exposure to PA57 enhances their defense capabilities. Our *in vivo* studies, using the air pouch model of PA57 infection in mice, further confirmed this hypothesis (Ciszek-Lenda et al. 2024). Transferring BG-trained macrophages not only reduced local bacterial proliferation but also inhibited the formation of extensive biofilm. Notably, lower serum levels of serum amyloid A and a reduced number of PA57 colony-forming units in the spleens of mice receiving trained macrophages indicate their anti-inflammatory effects and their capacity to reduce or eliminate bacteremia. We believe the most significant finding of these studies is the substantial impact of trained macrophages on the progression of PA57 infection (Ciszek-Lenda et al. 2024).

The aim of this study is to evaluate the effect of *S. cerevisiae* BG training on the response of murine macrophages to EPS derived from PA57, the main component of the *P. aeruginosa* biofilm. Importantly, both autocrine and paracrine properties of trained macrophages were analyzed. Furthermore, this study highlights the potential of BG-induced macrophage training as a therapeutic strategy to modulate the immune response and improve outcomes in bacterial biofilm infections.

2. Materials and Methods

2.1. Reagents

BG isolated from *S. cerevisiae* (Merck KGaA, Darmstadt, Germany) was used in this study. BG is a major structural component of the yeast cell wall, consisting predominantly of a β-1,3-linked glucan backbone with a limited number of β-1,6-linked branches. β-1,3-glucans are widely recognized as potent inducers of trained immunity and are considered one of the most effective agents for training innate immune cells, including macrophages (Chen et al. 2023), and indomethacin (INDO; both Merck KGaA).

2.2. Bacteria

All experiments in this study were performed using *P. aeruginosa* strain coded as PA57. Bacteria were isolated from the sputum of a patient during an exacerbation of the advanced stage of cystic fibrosis. PA57 had strong biofilm production capacity and was isolated from the patient with a severe form of the disease (Majka et al. 2021). Isolated bacteria were cultured in tryptic soy broth (Oxoid/ThermoFisher Scientific, Fremont, USA) for 72 h at 37°C under aerobic conditions. After cultivation, bacteria were centrifuged for 10 min at 500 g and washed with 10 mL of phosphate-buffered saline (PBS; pH 7.4, Sigma-Aldrich, Steinheim, Germany), then used for *in vivo* tests. For *in vitro* tests with immune cells, bacteria were killed (see below).

2.3. Killing *P. aeruginosa* bacterial cells

Bacterial pellets originating from 72 h cultures were treated thrice with high temperature (121°C) at 0.3 bars in the ASVE-ELMI ESS-207 SMS steam sterilizer and in that form were used to stimulate immune cells (see below). The follow-up bacterial culture was verified to be sterile.

2.4. Exopolysaccharide (EPS57) isolation

EPS57 was isolated and purified as described by Górska et al. (2014). Briefly, polysaccharide was obtained by trichloroacetic acid extraction of bacterial mass, precipitated

with ethanol, and purified by DNAse, RNAse, and protease. EPS57 was purified by ion-exchange chromatography. The fractions containing neutral EPS57 were pooled, desalted by dialysis against water at 4°C for 24 h, and lyophilized. Total saccharide concentration was measured by the phenol sulfuric acid method according to Dubois's method (Dubois et al. 1956).

2.5. Mice

Inbred C57BL/6 mice (8–12 weeks of age, 18–22 g) were maintained at the Animal Breeding Unit of the Department of Immunology of Jagiellonian University Medical College (Poland). All mice were held in standard caging conditions with water and standard diet *ad libitum*.

2.6. Cell isolation

For *in vitro* assays, peritoneal mouse exudate cells were induced by an intraperitoneal injection of 1.5 mL of 3% thioglycolate (Sigma-Aldrich). After 96 h (macrophages), mice were euthanized by isoflurane vapors (Abbott Laboratories, Illinois, USA), and cervical dislocation was performed. Cells were then collected by washing out the peritoneal cavity with 5 mL of PBS (Lonza, Verviers, Belgium) containing 5 U heparin/mL (Polfa, Warsaw, Poland). Cells were centrifuged, and red blood cells were lysed. Osmolarity was restored by the addition of PBS. At least two mice were used as donors of peritoneal exudate cells for each experiment.

2.7. Cell viability

Cell viability was monitored by means of lactate dehydrogenase (LDH) activity using LDH assay kit (Thermo Fisher Scientific) according to manufacturer's instructions. The viability of phagocytes was controlled in all experimental systems to avoid the cytotoxic effect of the tested agents.

2.8. Cell culture and treatment

Macrophages were cultured in 24-well flat-bottom cell culture plates at 5 × 10^5/well in IMDM medium (Lonza) supplemented with 5% fetal bovine serum (FBS; Lonza), 2 mM stable L-glutamine (Lonza), and 50 mg/mL gentamicin (Krka, Poland) at 37°C in an atmosphere of 5% CO_2. To train macrophages, cells were incubated for 24 h with 10 μg/mL of BG and then exposed to EPS57 (30 μg/mL) or/and selected bacteria (20:1 bacteria per cell). After 24 h of stimulation, culture supernatants were collected and frozen at −80°C until use. In some experiments, cells were preincubated with INDO (10 μM) for 30 min before BG was added.

2.9. Cytokine measurement

Cytokine levels in cell culture supernatants were measured by sandwich ELISA. Microtiter plates (Costar EIA/RIA plates, Corning, Inc., NY, USA) were coated with a cytokine-specific antibody. Expression levels of IL-6 and IL-10 were measured according to the manufacturer's instructions (OptEIA Sets, BD Biosciences, San Diego, USA). TNF-α level was measured according to the manufacturer's instructions (ELISA uncoated kits, Invitrogen, USA). In all cases, 10% FBS in PBS was used as a blocking solution. TMB substrate solution (Invitrogen, Waltham, USA) was used to develop a colorimetric reaction, which was stopped with 2 M sulfuric acid. Optical density was measured at 450 (570) nm using a microtiter plate reader (Power Wave X, Bio-Tek Instruments, Winooski, USA).

2.10. PGE_2 immunoassay

PGE_2 concentration in cell supernatants was determined by a PGE_2 high-sensitivity ELISA kit (Enzo Life Sciences, Farmingdale, USA), according to the manufacturer's protocol.

2.11. NO determination

Nitric oxide (NO) levels in culture supernatants of macrophages were quantified by the accumulation of nitrite as a stable end product, according to a modified Griess method (Ding et al. 1988). Cell culture supernatant (100 μL) was mixed with 14 mM 4,4′-diamino-diphenylsulphone (Dapsone, Sigma-Aldrich) in 2 M HCl (50 μL) and 0.1% N-1-naphtylenediamine dihydrochloride (50 μL) in deionized water. Absorbance of the tested culture supernatants at 550 nm was compared with a sodium nitrate standard ($NaNO_2$) curve.

2.12. Proteomics

2.12.1. Sample preparation for LC-MS/MS analysis

Macrophages were lysed in 150 μL of lysis buffer (2% SDS, 50 mM DTT in 0.1 M Tris-HCl, pH 7.6), vortexed, incubated in 95°C for 5 min, and clarified by centrifugation at 14 000 g for 30 min before protein digestion. The total protein concentration in collected lysates was determined by the WF-assay (Wiśniewski and Gaugaz 2015). Then, a volume containing 70 μg of total protein was transferred to Microcon-30kDa centrifugal filter units (Merck), denatured with 8 M urea in 0.1 M Tris-HCl, pH 8.5, and digested to peptides with the use of filter-aided sample preparation (FASP) protocol (Wiśniewski et al. 2009). Briefly, proteins were alkylated with iodoacetamide and cleaved with LysC-trypsin mix (Thermo Scientific, Waltham, MA, USA) with the enzyme to protein ratio1:50. Digestions were

carried out overnight in 50 mM Tris-HCl, pH 8.5, at 37°C. After digestion, the peptide yields were determined by WF-assay, and the aliquots containing equal amounts of total peptides were desalted on 96-Well MiniSpin C18 columns (Harvard Apparatus, Holliston, MA, USA). Samples were then concentrated to a volume of ~ 5 µL and stored at −80°C. For project-specific spectral libraries preparation, an equal number of peptides from 40 samples distributed across all experimental conditions were combined and subjected to a fractionation protocol. HpH-fractionation on C18 Micro SpinColumns (Harvard Apparatus) was performed in 50 mM ammonium formate buffer (pH 10) with 13 consecutive injections of the eluent buffer, comprising 5%, 10%, 12.5%, 15%, 17.5%, 20%, 22.5%, 25%, 27.5%, 30%, 35%, 50%, and 80% acetonitrile in 50 mM ammonium formate buffer (pH 10), collected by centrifugation (300 × *g*, 2 min) and dried in a speedvac concentrator (Eppendorf, Hamburg, Germany). In this way, peptides were distributed across 13 HpH fractions and analyzed by LC-MS/MS in DDA acquisition mode for library generation. Before the analysis, all samples and library peptide fractions were solubilized in 0.1% formic acid at a concentration of 0.5 µg/µL and spiked with the iRT peptide mix (Biognosys, Schlieren, Switzerland) for normalization of the retention time.

2.12.2. Liquid chromatography – tandem mass spectrometry

Peptides (1 µg) were injected onto a nanoEase M/Z Peptide BEH C18 75 µm i.d. × 25 cm column (Waters, Milford, MA, USA) *via* a trap column nanoEase M/Z Symmetry C18 180 µm i.d. × 2 cm column (Waters). For library generation, each peptide fraction was separated using a 98 min 1% to 40% B phase linear gradient (A phase: 0.1% FA; B phase: 80% ACN and 0.% FA) operating at a flow rate of 300 nL/min on an UltiMate 3000 HPLC system (Thermo Scientific) and applied to a TripleTOF 6600 + (Sciex, Framingham, MA, USA) mass spectrometer. The main working nanoelectrospray ion source (Optiflow, Sciex) parameters were as follows: ion spray voltage 3.2 kV, interface heater temperature 200°C, ion source gas 1 (GS1) 10, and curtain gas (CUR) 25. For DDA acquisition, spectra were collected in full scan mode (350–1400 Da), followed by 100 CID MS/MS scans of 100 most intense precursor ions from the preceding survey full scan exceeding 100 cps intensity under dynamic exclusion criteria. Samples analyzed in SWATH acquisition mode were separated using a 63 min 1%–40% B phase linear gradient at a flow rate of 300 nL/min. For SWATH acquisition, spectra were collected in full scan mode (400–1250 Da), followed by 100 SWATH MS/MS scans using a variable precursor isolation window approach, with m/z windows ranging 6–90 Da.

2.12.3. Mass spectrometric raw data analysis, spectral library generation, and SWATH quantitation

DDA data were searched against the murine UniProt database (release 2021_01_04, 17 056 entries) using the Pulsar search engine implemented in Spectronaut 18 software (Biognosys) (Bruderer et al. 2015) with default parameters (±40 ppm mass tolerance on MS1 and MS2 level, mutated decoy generation method, trypsin enzyme specificity). Deep Learning Assisted iRT Regression was set as the iRT reference strategy for RT to iRT calibration, with a minimum R2 set to 0.8. Peptide, protein, and Peptide-Spectrum Match/false discovery rate (FDR) were set to 1%. The library was generated using 3–6 fragment ions per precursor.

A project-specific library was then used to analyze the SWATH data in Spectronaut 18 (Biognosys). Data were filtered by 1% FDR on the peptide and protein level, while quantitation and interference correction were done on the MS2 level. Protein grouping was performed based on the ID picker algorithm (Zhang et al. 2007). Protein quantities were calculated by averaging the respective peptide intensities, while the latter were obtained as mean precursor quantities. The protein coefficients of variation were calculated based on the summed intensities of their respective peptides. Data were normalized using a global regression strategy, and statistical testing for differential protein abundance was performed using t-tests with multiple-testing correction as described by Storey (2002). Statistically significant differences (q value < 0.05) with a quantitative cut-off for an absolute 1.5-fold change were considered as differentially regulated. The details of differential protein abundances in comparisons between naïve controls, BG-trained, and EPS57-stimulated cells are collected in **Tables S1–S3**. The LC-MS data, library, and Spectronaut project have been deposited to the ProteomeXchange Consortium *via* the PRIDE partner repository (Perez-Riverol et al. 2024) with the dataset identifier PXD036521. Functional grouping and pathway annotations were performed using ClueGO (Bindea et al. 2009) under the Cytoscape 3.7.2 environment (Shannon et al. 2003) with the use of PINE software (Sundararaman et al. 2020). CORUM-3.0 (release 03.09.2018), KEGG (release 17.02.2020), REACTOME (release 17.02.2020), and WikiPathways (release 17.02.2020) pathway databases were used in the analysis. The enrichment results were validated by enrichment/depletion two-sided geometric statistical tests with the Benjamini-Hochberg *p-value* correction. The minimum and maximum GO levels were set at 3 and 8, respectively, with the cluster criterion of a minimum of three genes constituting a minimum of 4% of the GO term. The kappa score threshold was set to 0.4. The Partial Least Squares-Discriminant Analysis (PLS-DA) was performed in RStudio 2026.01.1 (Posit PBC, Boston, USA) (Build 403) using the mixOmics

package (Rohart et al., 2017), and the heatmap was generated using the pheatmap package.

2.13. Phagocytosis assay

Macrophages were seeded on 96-well plates (2 × 10^5 cells/well) and cultured in either regular medium or medium with BG (10 µg/mL). After 24 h, cells were washed twice with PBS, and a new medium was added to the respective groups: control medium, medium with EPS57, medium with PA57 (20:1 bacteria to macrophages ratio), or medium with both EPS57 and PA57. After another 24 h, cells were washed with PBS twice and then incubated for 90 min in 37°C without elevated CO_2 upon addition of pHrodo Red Bioparticles Conjugate (Thermo Fisher Scientific) according to manufacturer's instructions. Phagocytosis levels were evaluated using fluorescence measurements made with Tecan M200PRO plate reader (ex/em wavelengths of 560/585 nm, respectively).

2.14. Statistical analysis

Statistical significance of differences between groups was analyzed using one-way ANOVA, followed, if significant, by a Dunnett's test or Tukey's test for *post hoc* comparison. Results are expressed as mean ± SEM values. A p value < 0.05 was considered statistically significant. Analysis was performed using Graphpad Prism v. 5.01 (GraphPad Software, Inc., Boston, USA). The exact statistical analysis is named in the relevant figure's caption.

3. Results

3.1. Impact of EPS57 on the proteome of trained with BG macrophages *vs.* naïve macrophages

To assess how BG training modulates macrophage responses, we employed BG derived from *S. cerevisiae*. Our previous study established 10 µg/mL as the effective stimulatory concentration, inducing a pro-inflammatory mediator profile without triggering nitric oxide (NO) production (Ciszek-Lenda et al. 2024). Macrophages were therefore trained with BG for 24 h, followed by medium replacement and a secondary 24 h stimulation with EPS isolated from the PA57 biofilm or with whole killed bacteria.

To identify the molecular mechanisms underlying BG-induced reprogramming, we performed quantitative proteomic profiling of EPS57-stimulated macrophages. Overall, BG-trained macrophages showed moderate yet distinct proteomic changes upon EPS57 activation, with 82 proteins differentially regulated compared with naïve controls (Figures 1a,b,c, Table S1). Nevertheless, the changes observed at the level of whole proteomes allow for a clear separation of replicates in the PLS-DA analysis (Figure 1b). Pathway enrichment analysis revealed that these proteins were functionally enriched

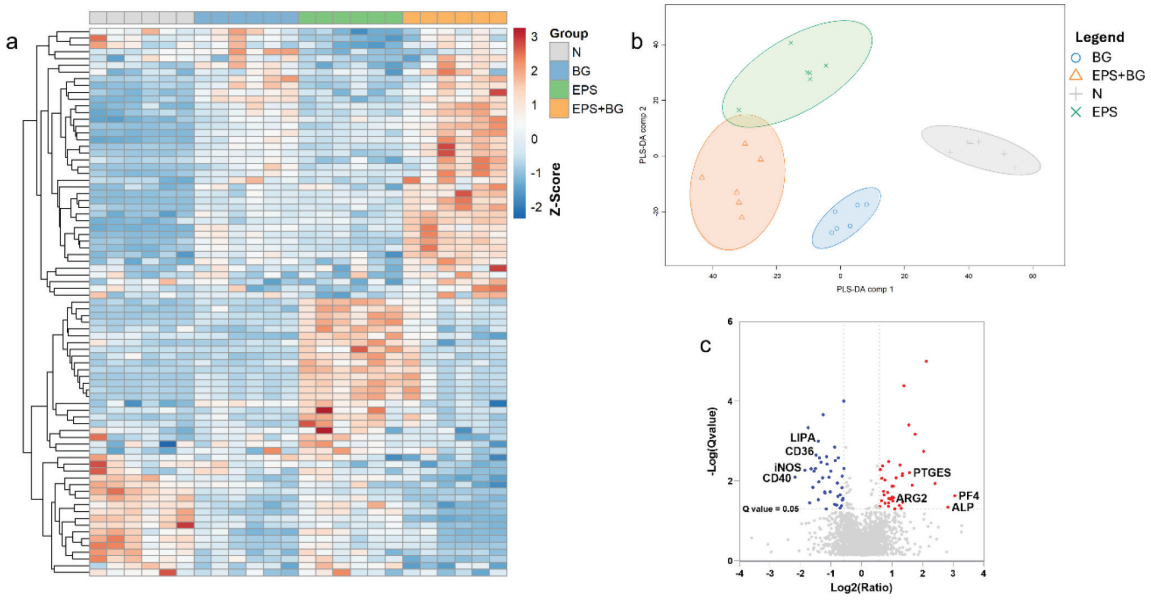

Fig 1. *An overview of the quantitative proteomics analyses. The regulated proteins exhibited marked differences in expression levels between naïve and BG-trained macrophages stimulated with EPS, as illustrated by the heatmap, which also includes unstimulated cells and those exposed to BG alone* ***(a)****. Based on whole-proteome profiles, PLS-DA enabled clear class separation between naïve and BG-trained macrophages, as well as between EPS-activated cells, highlighting the effects induced by BG training in EPS-stimulated specimens* ***(b)****. The volcano plot summarizes the quantitative differences between naïve and BG-trained macrophages stimulated with EPS and highlights proteins enriched in significantly altered pathways* ***(c)****. ALP, antileukoproteinase; BG, β-glucan; EPS, Exopolysaccharide; iNOS, inducible nitric oxide synthase; PLS-DA: partial least squares-discriminant analysis.*

74, 14 (2026), DOI: 10.2478/aite-2026-0014

in three interconnected modules: arginine biosynthesis, cholesterol metabolism, and arachidonic acid metabolism (Figures 2a and b), which has been described to regulate inducible nitric oxide synthase (iNOS) induction. Interestingly, proteins related to cholesterol transport and turnover are also regulated and evidence the induction of free cholesterol efflux machinery, as ATP binding cassette subfamily A member 1 (ABCA1) and LDL receptor related protein associated protein 1 are jointly upregulated (Figures 2a,b).

Importantly, our data point to several proteins with chemokine/cytokine functions that were regulated in response to BG training. The chemoattractant platelet factor 4 (PF4) was the protein with the highest (over eight-fold) abundance difference between BG-trained and naïve macrophages activated with EPS57 (Figure 2b). PF4 induction is the result of BG pretreatment and remains constant in EPS57-activated cells. Likewise, antileukoproteinase (ALP) follows the same expression pattern with over seven-fold induction in BG-trained cells as compared to the naïve controls (Figure 2b). Moreover, BG-trained macrophages induce complement C1q subcomponent subunit C (C1QC) (Table S1) in response to EPS57.

3.2. Effect of BG training on macrophage response to the EPS57 priming

3.2.1. Effect on macrophage secretory properties

Since the proteomic dataset indicated induction of PGE_2-associated enzymes (PLA2G4A and PTGES) and suppression of iNOS, we next examined whether these pathways are reflected in the secretory output of trained macrophages exposed to EPS57. Our experimental setup revealed that BG-trained macrophages displayed enhanced secretion of TNF-α, IL-6, and PGE_2 (Figure 3a-c), while IL-10 levels were reduced (Figure 3d) upon restimulation with EPS57. These findings indicate that BG training reprogrammed macrophages toward a pro-inflammatory response when interacting with EPS57. Interestingly, this training also resulted in a significant decrease in NO production following EPS57 restimulation (Figure 3e). Given that our secretome and proteome analyzes (Figure 2) revealed an increased expression of PGE_2 synthase and elevated PGE_2 secretion, accompanied by a concomitant downregulation of iNOS expression and NO production in BG-trained macrophages, we aimed to investigate whether this effect might be mediated by a secondary autocrine action of PGE_2. To test this hypothesis, cells were preincubated with INDO, a cyclooxygenase (COX)-2 inhibitor, before BG-training (Figures S1a,b). The results indicate that these effects are independent of COX-2 activity. INDO treatment did not significantly alter NO production in trained macrophages compared to cells subjected to BG-training alone (Figure S1b, blue bars *vs.* dark gray bars). These findings strongly suggest that the BG-induced reduction in iNOS expression is not mediated by COX-2-dependent PGE_2 production. However, further studies are required to elucidate the underlying mechanisms responsible for this phenomenon.

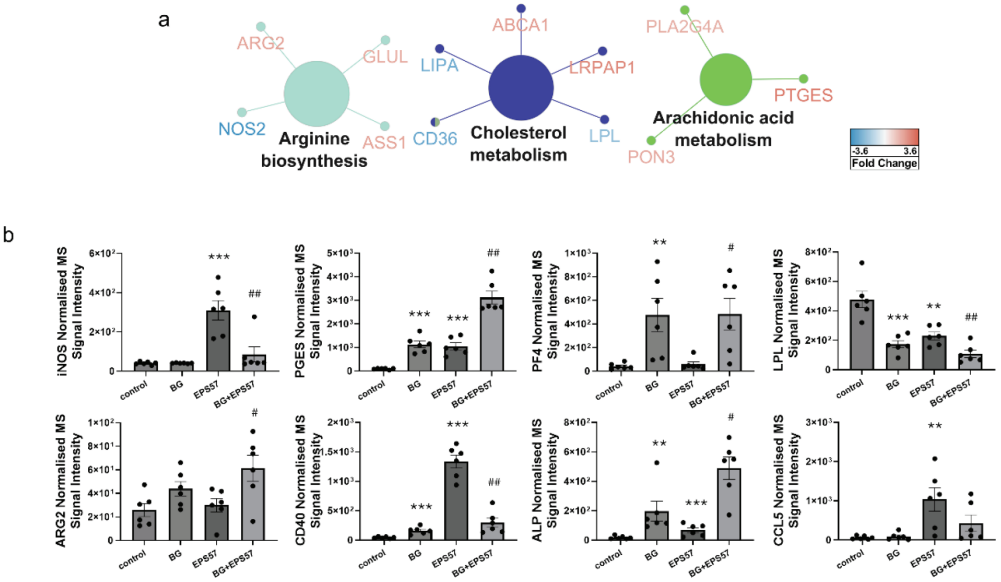

Fig 2. *Effect of BG training on EPS57-activated macrophages. Pathway enrichment analysis resulted in the identification of three functional modules in which the regulated proteins are engaged* ***(a)****. The normalized MS intensities derived from SWATH data for selected proteins* ***(b)*** *are presented as mean ± SEM values of n = 6 biological replicates. *p < 0.05, **p < 0.01, ***p < 0.001 indicate the significance of the difference observed with naïve controls; #p < 0.05, ##p < 0.01, ###p < 0.001 indicate BG-trained vs. BG-trained + EPS57. ALP, antileukoproteinase; BG, β-glucan.*

74, 14 (2026), DOI: 10.2478/aite-2026-0014

3.2.2. Effect on phagocytic properties

Since several differentially regulated proteins (PF4, ALP, and C1QC) are linked to macrophage effector functions and inflammatory tone, and because PGE_2/NO balance can influence phagocytic activity, we assessed whether BG-training affects the macrophage capacity to internalize particles. Evaluation of phagocytic activity of macrophages upon BG training and incubation with bacteria and/or biofilm components was based on comparison of fluorescence intensity of pH-sensitive fluorescently labeled zymosan particles. When macrophages were trained with BG before exposure to bacterial antigens (killed bacteria, purified), a statistically significant but modest (~10%) reduction in phagocytic capacity was observed (Figure S2). Given the small magnitude of this effect, we interpret this change as biologically limited rather than indicative of a strong functional impairment.

4. Discussion

Macrophages, the key effector cells of inflammation, exhibit remarkable phenotypic diversity, ranging from M1 (pro-inflammatory) to M2 (anti-inflammatory) phenotypes (Mills et al. 2000). Both functional types can play a dual role in innate immunity, beneficial as well as detrimental. Specifically, M1 macrophages are involved in pathogen killing and eradication but can also contribute to tissue damage (Gordon and Taylor 2005; Locati et al. 2020). In contrast, M2 macrophages participate in tissue repair, resolution of inflammation, and promotion of wound healing; however, as tumor-associated macrophages, they can also facilitate cancer progression (Mantovani 2014). Notably, biofilm-forming *P. aeruginosa* strains may evade phagocytosis and elimination while simultaneously inducing a hyperinflammatory macrophage phenotype, referred to as biofilm-associated macrophages (Strus et al. 2015; Ciszek-Lenda et al. 2019). These opposing properties arise from distinct macrophage microenvironments and diverse stimuli that lead to the production of different effector molecules.

Unlike classical M1/M2 polarization, trained macrophages arise through a process termed trained immunity, in which innate immune cells undergo long-term functional reprogramming following a primary stimulus, leading to enhanced responsiveness upon secondary challenge. This process does not involve antigen-specific memory but is driven by epigenetic and metabolic reprogramming. Stimuli, such as BG (derived from *S. cerevisiae*), the Bacillus Calmette-Guérin vaccine, or specific microbial components, can induce this state. Generally, trained macrophages exhibit heightened cytokine production (e.g., TNF-α, IL-6, and IL-1β) and increased phagocytic and antimicrobial activity upon restimulation, even against unrelated pathogens (Murphy et al. 2020; Chen et al. 2023).

In this study, we investigated the effects of BG-induced training on macrophages and their subsequent responses to EPS, the major inducers of detrimental and ineffective biofilm-associated macrophages (Ciszek-Lenda et al. 2023). We aimed to elucidate

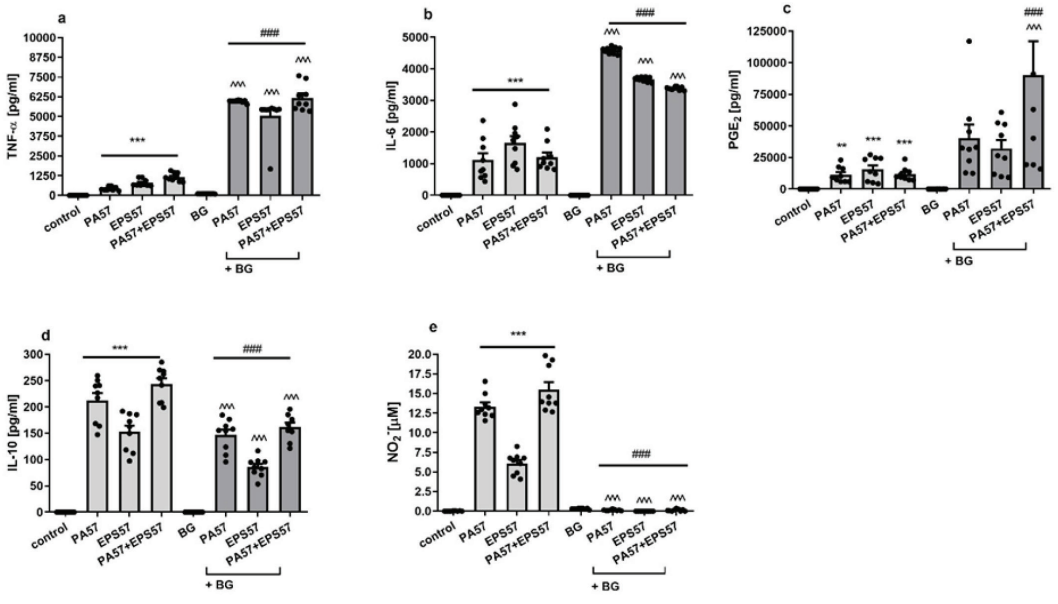

*Fig 3. Secretory properties of BG-trained macrophages exposed to EPS57. Levels of TNF-α **(a)**, IL-6 **(b)**, PGE_2 **(c)**, IL-10 **(d)**, and NO **(e)** were analyzed by ELISA or Griess method, respectively, in supernatants collected 24 h after the restimulation of macrophages with EPS57/killed bacteria. Data are mean ± SEM values of three independent experiments (macrophages isolated from three mice and tested in three technical replicates, n = 9), $^{**}p < 0.01$ and $^{***}p < 0.001$ not trained vs. control; ###$p < 0.001$ trained vs. BG; ^^^$p < 0.001$ trained vs. not trained. BG, β-glucan; IL, interleukin; NO, nitric oxide; PGE_2: prostaglandin E_2; TNF-α, tumor necrosis factor-α.*

the potential autocrine and paracrine activities of BG-trained macrophages, particularly the mechanisms underlying the strong anti-biofilm effects previously observed in *P. aeruginosa* (PA57)-infected mice (Ciszek-Lenda et al. 2024).

Herein, in our experimental setting, BG stimulation markedly enhanced the production of proinflammatory mediators, including TNF-α, IL-1, IL-6, and PGE_2. Unexpectedly, this response was accompanied by a profound suppression of NO synthesis and a reduction in phagocytic capacity in EPS57 restimulated macrophages. Furthermore, BG training resulted in significant downregulation of lipoprotein lipase (LPL). LPL plays a complex role in macrophage polarization, primarily through LPL-mediated lipid uptake and subsequent activation of peroxisome proliferator-activated receptors, which promote fatty acid oxidation and drive the development of anti-inflammatory phenotypes (Hiemstra et al. 1996). These findings suggest that BG-trained macrophages may acquire adverse or functionally disadvantageous properties, potentially impairing their effectiveness in host defense against bacterial biofilm infections. Proteomic analysis, however, revealed a concomitant upregulation of ALP, an enzyme with both antimicrobial and anti-proteolytic activities. In macrophages, ALP secretion contributes to both direct pathogen killing and modulating the inflammatory response to infection (Benoit et al. 2012). The N-terminal domain of ALP exerts direct antimicrobial effects, whereas the C-terminal domain inhibits proteases such as neutrophil elastase, which contribute to inflammatory tissue injury (Chang et al. 2019). This mechanism may partially compensate for the reduced NO production and the minor reduction in phagocytic capacity observed in BG-trained macrophages. Nevertheless, the most promising outcome of BG training appears to be the induction of mediators that enhance the paracrine activity of macrophages at sites of inflammation, including PF4, selected chemokines (e.g., Ccl5), C1QC, and PGE_2. Specifically:

i) PF4 interacts with bacteria to augment host-defense functions and improve outcomes in severe bacterial infections, including sepsis. For example, PF4 has been reported to enhance bacterial capture by neutrophil extracellular traps and improve survival in murine LPS-induced endotoxemia (Ngo et al. 2023).
ii) C-C motif chemokine 5 (Ccl5, RANTES) plays a dual role in bacterial infections: it acts as a chemoattractant that recruits macrophages and neutrophils to infection sites and promotes paracrine, proinflammatory macrophage activity. However, excessive CCL5 production, particularly during viral-bacterial coinfections, may exacerbate inflammation and contribute to cytokine storm syndromes (Hwaiz et al. 2015).
iii) C1QC functions beyond complement activation and behaves as an anti-inflammatory cytokine-like mediator and promotes M2-like macrophage polarization, enhances apoptotic cell clearance, playing an important role in immune resolution and tissue homeostasis (Benoit et al. 2012).
iv) PGE_2 is a major macrophage-derived eicosanoid that exerts both pro- and anti-inflammatory effects, depending on the cellular context and signaling milieu (Loynes et al. 2018). Notably, PGE_2 has been shown to promote neutrophil apoptosis and efferocytosis processes associated with the resolution of inflammation (Schmid and Brüne 2021). However, the effect of PGE_2 on neutrophil apoptosis can be beneficial or detrimental, depending on the infection phase.

Importantly, some chemotactic properties of these selected paracrine factors may explain the beneficial effects of BG–trained macrophages transferred into mice infected with *P. aeruginosa* (PA57), as it has been shown in our previous studies (Ciszek-Lenda et al. 2024). In those studies, we observed a significant reduction in bacterial proliferation and biofilm formation, accompanied by increased infiltration of endogenous neutrophils and macrophages (Ciszek-Lenda et al. 2023, 2024). These findings suggest that such trained macrophages facilitate the recruitment of naïve phagocytes to the site of inflammation.

Furthermore, the enhanced production of PGE_2, accompanied by a marked reduction in NO generation, appears to be a hallmark of our trained macrophages ($M\phi^{high}PGE_2/^{low}NO$). Further investigation is required to determine whether this mediator profile exerts beneficial or detrimental effects during bacterial infection.

Notably, PGE_2 and inducible iNOS are both critical regulators of macrophage function, but their interplay is complex and context dependent. PGE_2 can either promote or inhibit iNOS expression and activity, depending on the cellular environment and nature of the activating stimuli (Posadas et al. 2000; Dahiya et al. 2010). Conversely, other studies have demonstrated that attenuation of iNOS expression in LPS-stimulated macrophages occurs independently of COX-2-derived PGE_2 (Razzak et al. 2008). Our findings are consistent with this observation: the reduced NO production in trained macrophages treated with INDO was comparable to that in trained macrophages exhibiting elevated PGE_2 levels. These results suggest that, at sites of inflammation, EPS-stimulated trained macrophages may secrete high levels of PGE_2 without concomitant NO production. Whether this mediator profile offers an advantage compared to the simultaneous high PGE_2 and NO production observed in non-trained macrophages remains an open question.

During the early stages of bacterial infection, PGE_2 and NO often act synergistically to modulate vascular tone, enhance local blood flow, and promote immune cell recruitment to sites of infection, thereby facilitating pathogen clearance (Martínez-Colón and Moore 2018). However,

74, 14 (2026), DOI: 10.2478/aite-2026-0014

when excessively produced, both mediators can suppress immune responses and contribute to bacterial persistence. Specifically, PGE_2 inhibits Th1 cytokine production (e.g., IFN-γ, IL-12), thereby impairing bacterial clearance, while high levels of NO can inhibit T-cell proliferation and mitochondrial function and induce tissue damage *via* nitrosative stress (Allione et al. 1999). Additionally, premature neutrophil apoptosis may further compromise bacterial elimination. Excessive PGE_2, as observed during certain infections, such as Mycobacterium tuberculosis, can suppress innate immune responses (Chen et al. 2008).

In contrast, during the later stages of infection or in recurrent bacterial infections, elevated PGE_2 levels may facilitate macrophage and dendritic cell migration, tissue repair, and resolution of inflammation (Ortega-Gómez et al. 2013; Davis et al. 2020). PGE_2-mediated apoptosis plays an essential role in controlling inflammation and promoting tissue repair by enhancing efferocytosis and driving anti-inflammatory macrophage polarization. For instance, in *P. aeruginosa* lung infection, PGE_2 limits neutrophil lifespan, thereby reducing tissue damage. Consequently, BG-trained macrophages may exert beneficial effects in chronic biofilm-associated bacterial infections, including *P. aeruginosa* lung infections in cystic fibrosis (Table 1).

5. Conclusions

Proteomic analyzes collectively indicate that the phenotype of *S. cerevisiae* BG-induced macrophages exhibit a mixed pro- and anti-inflammatory profile initiated in response to EPS57 activation. Importantly, this study, together with previous reports, suggests that the final phenotype of trained macrophages can vary substantially depending on the specific induction conditions, ranging from an M1-like pro-inflammatory to an M2-like anti-inflammatory state.

Our findings further highlight the therapeutic potential of BG–trained macrophages characterized by elevated PGE_2 secretion and markedly reduced NO production (Mϕ–$^{high}PGE_2$/^{low}NO). However, during acute bacterial infections accompanied by local inflammation, tissue-resident and infiltrating monocyte-derived macrophages play a critical role in pathogen clearance and the subsequent resolution of inflammation:

i. Early stages of acute infection – During pathogen adherence and the onset of acute inflammation, M1-like pro-inflammatory and microbicidal macrophages cooperate with neutrophils to eliminate planktonic bacteria.
ii. Late stages of acute infection – During the resolution phase of infection and inflammation, M2-like anti-inflammatory and pro-resolving macrophages protect host tissues from excessive or chronic inflammation.
iii. Chronic infection – Macrophages located in proximity to biofilms often exhibit impaired phagocytic activity and dysregulated cytokine production, thereby promoting persistent inflammation without effective bacterial clearance. Moreover, hyperinflammatory neutrophils and macrophages contribute to local tissue damage.

Therefore, during acute infections, the induction or administration of trained macrophages to further enhance innate immune responses appears inadvisable, as it may interfere with the natural progression of inflammation and pathogen elimination.

Conversely, in chronic or recurrent *P. aeruginosa* biofilm-associated infections—such as those occurring in cystic fibrosis

Table 1. *Roles of PGE_2 and NO in the inflammatory functions of M1, M2, and trained macrophages*

Feature	M1 macrophages (classically activated)	M2 macrophages (alternatively activated)	Trained macrophages ($^{high}PGE_2$/^{low}NO)
Activation stimuli	LPS, IFN-γ, TNF-α	IL-4, IL-13, IL-10, glucocorticoids	*S. cerevisiae* BG
COX-2 expression/PGE_2 secretion	**High/High**	**Low-moderate/low**	**High/high**
Functional role of PGE_2	Pro-inflammatory; promotes IL-6, IL-1β	Anti-inflammatory; promotes tissue repair, fibrosis	Promotes neutrophil apoptosis and efferocytosis. Tissue repair.
iNOS	**Strongly induced**	**Weak or absent**	**Weak or absent**
NO production	**High** (major molecule for pathogen killing)	**Low** (minimal cytotoxic activity)	**Low** (minimal cytotoxic activity)
Functional role of NO	Microbicidal; contributes to oxidative stress	Suppresses inflammation; promotes healing indirectly (low NO maintains tissue integrity)	Suppresses inflammation; promotes healing indirectly (low NO maintains tissue integrity)
Beneficial functions	Early stages of infection/inflammation. Cooperation with neutrophils in pathogen killing	Resolution of inflammation. Efferocytosis of apoptotic neutrophils	Late stages of infection/inflammation. Recruitment of naïve macrophages. Resolution of chronic inflammation. Reduction of hyperinflammatory response

BG, β-glucan; COX, cyclooxygenase; IL, interleukin; iNOS, inducible nitric oxide synthase; LPS, lipopolysaccharides; NO, nitric oxide; PGE_2, prostaglandin E_2; TNF-α, tumor necrosis factor-α.

lungs or non-healing wounds—where macrophage access to bacteria embedded within the biofilm matrix is restricted, therapeutic strategies should aim to mitigate tissue injury driven by hyperinflammation. Under such conditions, the use of trained macrophages with high PGE_2 and low NO output (Mϕ–$^{high}PGE_2$/^{low}NO), exhibiting anti-inflammatory, proapoptotic, and chemotactic effects on resident naïve macrophages, represents a promising therapeutic approach. In these settings, indirect effects mediated through neighboring and infiltrating immune cells are likely to play a pivotal role.

Moreover, the prophylactic induction of trained immunity may prove beneficial in reducing susceptibility to infections, particularly those for which effective vaccines are not yet available. Nevertheless, further studies are required to establish optimized protocols for *in vivo* BG-induced macrophage training, including potential integration with probiotic administration. Notably, *S. cerevisiae* represents a unique microbial stimulus capable of bridging probiotic function and innate immune training, thereby offering promising opportunities for infection control and immunotherapy.

In conclusion, the development of novel strategies to enhance innate immunity through trained macrophages is essential for strengthening both individual and herd-trained immunity (Marcinkiewicz 2025). However, treatment with trained or engineered macrophages is not currently recommended as standard therapy. Although this approach represents a promising area of research, its application should be restricted to clinical trials until safety and efficacy are firmly established. Nevertheless, BG has already been administered in human medicine and has demonstrated beneficial effects in patients with impaired immunity, particularly those experiencing recurrent infections. However, these effects have largely lacked a clear mechanistic explanation (Horneck Johnston et al. 2024). Our findings may at least partially elucidate the beneficial role of BG by identifying it as a major driver of trained immunity.

Funding

This study was supported by the National Science Center, Poland (Grant no. 2017/27/B/NZ6/001772). The funders had no role in study design, data collection and analysis, decision to publish, or preparation of the manuscript.

Acknowledgments

The authors would like to thank Paulina Skalska for her skillful technical assistance.

Statement of Ethics

This study was carried out in strict accordance with recommendations from the Guide for the Care and Use of Laboratory Animals of the Ministry of Science and Information of Poland. The protocol was approved by the Local Committee on the Ethics of Animal Experiments of Jagiellonian University (941/2024) and by the Local Bioethics Committee (decision number 1072.6120.252.2018).

Conflict of Interest Statement

The authors declare no conflict of interest.

Authorship

JM, MCL, and GM conceived and designed experiments. BN, MCL, GM, MS, IS, ED, and SG performed the experiments. BN, MCL, GM, JM, and MS analyzed the results. JM, MCL, MS, and GM wrote the manuscript. RO and MStrus critically read the manuscript. All authors read and approved the final manuscript.

Data Availability Statement

All data generated or analyzed during this study are included in this article. Further inquiries can be directed to the corresponding author.

Supplementary Material

The Supplementary Material for this article can be found online at: Additional materials (tables) are available from the author upon request.

References

Allione A, Bernabei P, Bosticardo M et al. (1999) Nitric oxide suppresses human T lymphocyte proliferation through IFN-γ-dependent and IFN-γ-independent induction of apoptosis. J Immunol 163: 4182–4191. https://doi.org/10.4049/jimmunol.163.8.4182

Benoit ME, Clarke EV, Morgado P et al. (2012) Complement protein C1q directs macrophage polarization and limits inflammasome activity during the uptake of apoptotic cells. J Immunol 188:5682–5693. https://doi.org/10.4049/jimmunol.1103760

Bindea G, Mlecnik B, Hackl H et al. (2009) ClueGO: A cytoscape plug-in to decipher functionally grouped gene ontology and pathway annotation networks. Bioinformatics 25:1091–1093. https://doi.org/10.1093/bioinformatics/btp101

Bruderer R, Bernhardt OM, Gandhi T et al. (2015) Extending the limits of quantitative proteome profiling with data-independent acquisition and application to acetaminophen-treated three-dimensional liver microtissues. Mol Cell Proteomics 14:1400–1410. https://doi.org/10.1074/mcp.M114.044305

Carey JN, Lamont S, Wozniak DJ et al. (2024) Quorum sensing regulation of Psl polysaccharide production by *Pseudomonas aeruginosa*. J Bacteriol 206:e00312–00324. https://doi.org/10.1128/jb.00312-24

Chang HR, Josefs T, Scerbo D et al. (2019) Role of LPL (lipoprotein lipase) in macrophage polarization *in vitro* and *in vivo*. Arterioscler Thrombo Vasc Biol 39:1967–1985. https://doi.org/10.1161/ATVBAHA.119.312389

Chen J, Gao L, Wu X et al. (2023) BCG-induced trained immunity: History, mechanisms and potential applications. J Transl Med 21:106. https://doi.org/10.1186/s12967-023-03944-8

Chen M, Divangahi M, Gan H et al. (2008) Lipid mediators in innate immunity against tuberculosis: Opposing roles of PGE2 and LXA4 in the induction of macrophage death. J Exp Med 205:2791–2801. https://doi.org/10.1084/jem.20080767

Chung J, Eisha S, Park S et al. (2023) How three self-secreted biofilm exopolysaccharides of *Pseudomonas aeruginosa*, Psl, Pel, and alginate, can each be exploited for antibiotic adjuvant effects in cystic fibrosis lung infection. Int J Mol Sci 24:8709. https://doi.org/10.3390/ijms24108709

Ciszek-Lenda M (2011) Biological functions of exopolysaccharides from probiotic bacteria. Centr Eur J Immunol 36:51–55.

Ciszek-Lenda M, Majka G, Suski M et al. (2023) Biofilm-forming strains of *P. aeruginosa* and *S. aureus* isolated from cystic fibrosis patients differently affect inflammatory phenotype of macrophages. Inflamm Res 72:1275–1289. https://doi.org/10.1007/s00011-023-01743-x

Ciszek-Lenda M, Nowak B, Majka G et al. (2024) *Saccharomyces cerevisiae* β-glucan improves the response of trained macrophages to severe *P. aeruginosa* infections. Inflamm Res 73:1283–1297. https://doi.org/10.1007/s00011-024-01898-1

Ciszek-Lenda M, Strus M, Walczewska M et al. (2019) *Pseudomonas aeruginosa* biofilm is a potent inducer of phagocyte hyperinflammation. Inflamm Res 68:397–413. https://doi.org/10.1007/s00011-019-01227-x

Dagenais A, Villalba-Guerrero C, Olivier M (2023) Trained immunity: A “new” weapon in the fight against infectious diseases. Front Immunol 14:1147476. https://doi.org/10.3389/fimmu.2023.1147476

Dahiya Y, Pandey RK, Bhatt KH et al. (2010) Role of prostaglandin E2 in peptidoglycan mediated iNOS expression in mouse peritoneal macrophages *in vitro*. FEBS Lett 584:4227–4232. https://doi.org/10.1016/j.febslet.2010.09.009

Davis FM, Tsoi LC, Wasikowski R et al. (2020) Epigenetic regulation of the PGE2 pathway modulates macrophage phenotype in normal and pathologic wound repair. JCI Insight 5:e138443. https://doi.org/10.1172/jci.insight.138443

Ding AH, Nathan CF, Stuehr DJ (1988) Release of reactive nitrogen intermediates and reactive oxygen intermediates from mouse peritoneal macrophages. Comparison of activating cytokines and evidence for independent production. J Immunol 141:2407–2412. https://doi.org/10.4049/jimmunol.141.7.2407

Dubois M, Gilles KA, Hamilton JK et al. (1956) Colorimetric method for determination of sugars and related substances. Anal Chem 28:350–356. https://doi.org/10.1021/ac60111a017

El-Mahdy OM, Mohamed HI, El-Ansary AE (2023) Optimizations of exopolysaccharide production by *Fusarium nygamai* strain AJTYC1 and its potential applications as an antioxidant, antimicrobial, anticancer, and emulsifier. BMC Microbiol 23:345. https://doi.org/10.1186/s12866-023-03100-8

Gordon S, Taylor PR (2005) Monocyte and macrophage heterogeneity. Nat Rev Immunol 5:953–964. https://doi.org/10.1038/nri1733

Górska S, Schwarzer M, Jachymek W et al. (2014) Distinct immunomodulation of bone marrow-derived dendritic cell responses to *Lactobacillus plantarum* WCFS1 by two different polysaccharides isolated from *Lactobacillus rhamnosus* LOCK 0900. Appl Environ Microbiol 80:6506–6516. https://doi.org/10.1128/AEM.02104-14

Hiemstra PS, Maassen RJ, Stolk J et al. (1996) Antibacterial activity of antileukoprotease. Infect Immun 64:4520–4524. https://doi.org/10.1128/iai.64.11.4520-4524.1996

Horneck Johnston CJH, Ledwith AE, Lundahl MLE et al. (2024) Recognition of yeast β-glucan particles triggers immunometabolic signaling required for trained immunity. iScience 27:109030. https://doi.org/10.1016/j.isci.2024.109030

Hwaiz R, Rahman M, Syk I et al. (2015) Rac1-dependent secretion of platelet-derived CCL5 regulates neutrophil recruitment via activation of alveolar macrophages in septic lung injury. J Leukoc Biol 97:975–984. https://doi.org/10.1189/jlb.4A1214-603R

Li C, Wang H, Zhu B et al. (2024) Polysaccharides and oligosaccharides originated from green algae: Structure, extraction, purification, activity and applications. Bioresour Bioprocess 11:85. https://doi.org/10.1186/s40643-024-00800-5

Locati M, Curtale G, Mantovani A (2020) Diversity, mechanisms, and significance of macrophage plasticity. Annu Rev Pathol 15:123–147. https://doi.org/10.1146/annurev-pathmechdis-012418-012718

Loynes CA, Lee JA, Robertson AL et al. (2018) PGE2 production at sites of tissue injury promotes an anti-inflammatory neutrophil phenotype and determines the outcome of inflammation resolution *in vivo*. Sci Adv 4:eaar8320. https://doi.org/10.1126/sciadv.aar8320

Majka G, Mazurek H, Strus M et al. (2021) Chronic bacterial pulmonary infections in advanced cystic fibrosis differently affect the level of sputum neutrophil elastase, IL-8 and IL-6. Clin Exp Immunol 205:391–405. https://doi.org/10.1111/cei.13624

Mantovani A (2014) Macrophages, neutrophils, and cancer: A double edged sword. New J Sci 2014:271940. https://doi.org/10.1155/2014/271940

Marcinkiewicz J (2025) Post-pandemic upsurge of group A streptococcus infections: Potential link to impaired herd trained immunity following COVID-19 lockdowns. Front Immunol 16:1684332. https://doi.org/10.3389/fimmu.2025.1684332

Martínez-Colón GJ, Moore BB (2018) Prostaglandin E2 as a regulator of immunity to pathogens. Pharmacol Ther 185:135–146. https://doi.org/10.1016/j.pharmthera.2017.12.008

Mills CD, Kincaid K, Alt JM et al. (2000) M-1/M-2 macrophages and the Th1/Th2 paradigm. J Immunol 164:6166–6173. https://doi.org/10.4049/jimmunol.164.12.6166

Murphy EJ, Rezoagli E, Major I et al. (2020) β-Glucan metabolic and immunomodulatory properties and potential for clinical application. J Fungi 6:356. https://doi.org/10.3390/jof6040356

Ngo ATP, Levine N, Skidmore AE et al. (2023) Platelet factor 4 enhances antimicrobial function of the endothelium and improves outcome in a murine model of sepsis. Blood 142:1198. https://doi.org/10.1182/blood-2023-186989

Ochando J, Mulder WJM, Madsen JC et al. (2023) Trained immunity — basic concepts and contributions to immunopathology. Nat Rev Nephrol 19:23–37. https://doi.org/10.1038/s41581-022-00633-5

Ortega-Gómez A, Perretti M, Soehnlein O (2013) Resolution of inflammation: An integrated view. EMBO Mol Med 5:661–674. https://doi.org/10.1002/emmm.201202382

Perez-Riverol Y, Bandla C, Kundu Deepti J et al. (2024) The PRIDE database at 20 years: 2025 update. Nucl Acids Res 53: D543–D553. https://doi.org/10.1093/nar/gkae1011

Pompilio A, Crocetta V, De Nicola S et al. (2015) Cooperative pathogenicity in cystic fibrosis: *Stenotrophomonas maltophilia* modulates *Pseudomonas aeruginosa* virulence in mixed biofilm. Front Microbiol 6:951. https://doi.org/10.3389/fmicb.2015.00951

Posadas I, Terencio MC, Guillén I et al. (2000) Co-regulation between cyclo-oxygenase-2 and inducible nitric oxide synthase expression in the time-course of murine inflammation. Naunyn Schmiedeberg's Arch Pharmacol 361:98–106. https://doi.org/10.1007/s002109900150

Razzak A, Aldrich C, Babcock TA et al. (2008) Attenuation of iNOS in an LPS-stimulated macrophage model by omega-3 fatty acids is independent of COX-2 derived PGE2. J Surg Res 145:244–250. https://doi.org/10.1016/j.jss.2007.07.003

Rohart F, Gautier B, Singh A et al. (2017) mixOmics: An R package for omics feature selection and multiple data integration. PLoS Comput Biol 13:e1005752. https://doi.org/10.1371/journal.pcbi.1005752

Schmid T, Brüne B (2021) Prostanoids and resolution of inflammation – beyond the lipid-mediator class switch. Front Immunol 12:714042. https://doi.org/10.3389/fimmu.2021.714042

Shannon P, Markiel A, Ozier O et al. (2003) Cytoscape: A software environment for integrated models of biomolecular interaction networks. Genome Res 13:2498–2504. https://doi.org/10.1101/gr.1239303

Storey JD (2002) A direct approach to false discovery rates. J Royal Statist Soc Series B: Statist Methodol 64:479–498. https://doi.org/10.1111/1467-9868.00346

Strus M, Walczewska M, Machul A et al. (2015) Taurine haloamines and biofilm. Part I: Antimicrobial activity of taurine bromamine and chlorhexidine against biofilm forming *Pseudomonas aeruginosa*. Adv Exp Med Biol 803:121–132. https://doi.org/10.1007/978-3-319-15126-7_11

Sundararaman N, Go J, Robinson AE et al. (2020) PINE: An automation tool to extract and visualize protein-centric functional networks. J Am Soc Mass Spectrom 31:1410–1421. https://doi.org/10.1021/jasms.0c00032

Vestby LK, Grønseth T, Simm R et al. (2020) Bacterial biofilm and its role in the pathogenesis of disease. Antibiotics 9:59. https://doi.org/10.3390/antibiotics9020059

Wang W, Ju Y, Liu N et al. (2023) Structural characteristics of microbial exopolysaccharides in association with their biological activities: A review. Chem Biol Technol Agric 10:137. https://doi.org/10.1186/s40538-023-00515-3

Wiśniewski JR, Gaugaz FZ (2015) Fast and sensitive total protein and peptide assays for proteomic analysis. Anal Chem 87: 4110–4116. https://doi.org/10.1021/ac504689z

Wiśniewski JR, Zougman A, Nagaraj N et al. (2009) Universal sample preparation method for proteome analysis. Nat Methods 6:359–362. https://doi.org/10.1038/nmeth.1322

Zhang B, Chambers MC, Tabb DL (2007) Proteomic parsimony through bipartite graph analysis improves accuracy and transparency. J Proteome Res 6:3549–3557. https://doi.org/10.1021/pr070230d

Zhong X, Wang G, Li F et al. (2023) Immunomodulatory effect and biological sgnificance of β-glucans. Pharmaceutics 15:1615. https://doi.org/10.3390/pharmaceutics15061615

74, 14 (2026), DOI: 10.2478/aite-2026-0014

Supplementary Materials

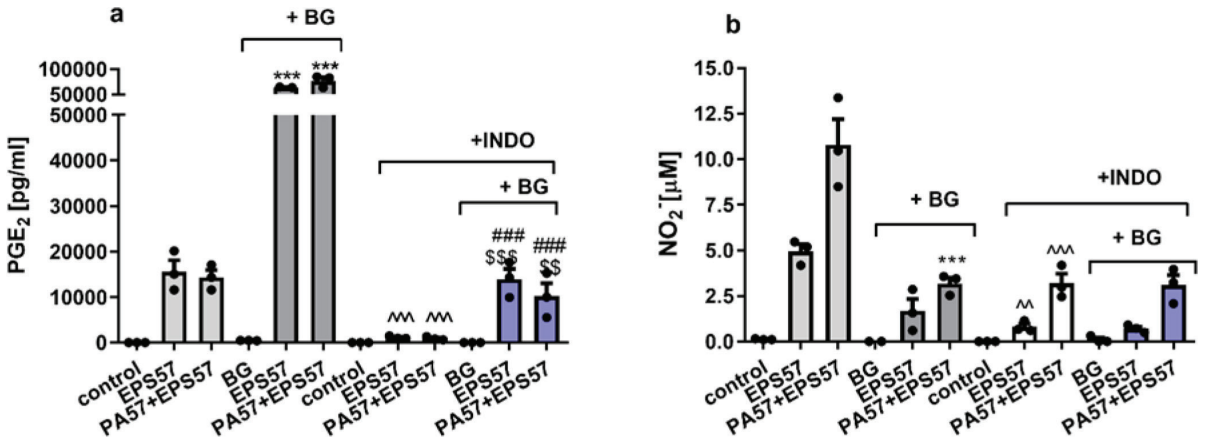

Fig S1. *Influence of indomethacin on PGE_2 and NO secretion in BG-trained macrophages exposed to EPS57. Levels of PGE_2* ***(a)*** *and NO* ***(b)*** *were analyzed by ELISA or Griess method, respectively, in supernatants collected 24 h after the restimulation of macrophages with EPS57/killed bacteria in the presence or absence of indomethacin (10 µM). Data are mean ± SEM values of three independent technical replicates. $^{***}p < 0.001$ not trained vs. trained; $^{###}p < 0.001$ trained vs. trained + INDO; $^{\wedge\wedge}p < 0.01$ and $^{\wedge\wedge\wedge}p < 0.001$ not trained vs. not trained + INDO; $^{\$\$}p < 0.01$ and $^{\$\$\$}p < 0.001$ not trained + INDO vs. trained + INDO. BG, β-glucan; NO, nitric oxide; PGE_2, prostaglandin E_2.*

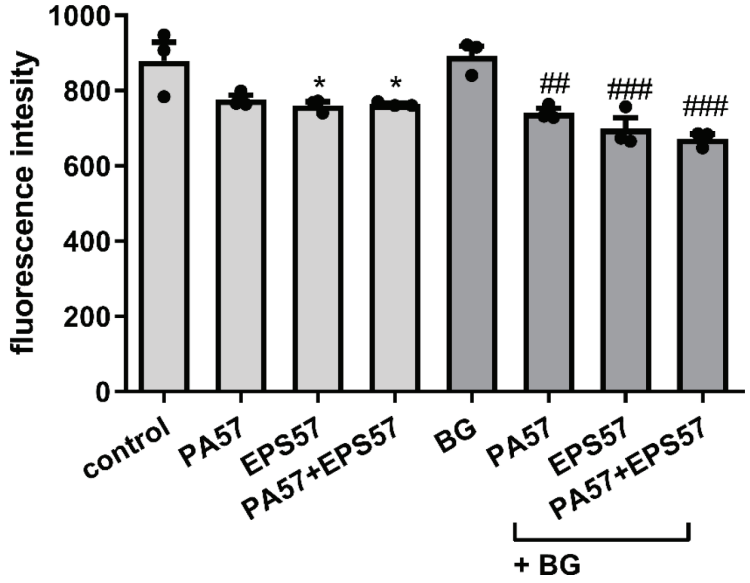

Fig S2. *Phagocytic properties of BG-trained macrophages exposed to EPS57 or killed bacteria. Intensity of fluorescence corresponding to phagocytic activity levels was assessed upon 90 min of incubation with fluorescently labeled zymosan particles. Data are mean ± SEM values of three independent experiments. Each group was run in four technical replicates. $*p < 0.05$ not trained vs. control; $^{##}p < 0.01$ $^{###}p < 0.001$ trained vs. BG. BG, β-glucan.*

Supplementary Table S1. *Differentially regulated proteins in β-glucan-treated and naïve macrophages activated with EPS57.*

Supplementary Table S2. *Differentially regulated proteins in β-glucan-treated and naïve macrophages.*

Supplementary Table S3. *Differentially regulated proteins in EPS57-activated macrophages and naïve controls.*